ЖУРНАЛ СТРУКТУРНОЙ ХИМИИ

2017. Том 58, № 8 *Ноябрь – декабрь* *С. 1610 – 1616*

UDC 547.945:548.737

STRUCTURE, DNA BONDING, AND BIOLOGICAL ACTIVITY OF A NOVEL Pb(II) COMPLEX OF 1,1-BIS(5-(PYRAZIN-2-YL)-1,2,4-TRIAZOL-3-YL) METHANE

E.-J. Gao, B. Meng, J.-Q. Su, T.-T. Peng, Z.-Z. Qi, B. Jia, Y.-H. Feng, M.-C. Zhu

Key Laboratory of the Inorganic Molecule-Based Chemistry of Liaoning Province and Laboratory of Coordination Chemistry, Shenyang University of Chemical Technology, Shenyang, P.R. China
E-mail: enjungao@163.com or mczhu@syuct.edu.cn

Received March, 7, 2016

A novel complex $[Pb(bptm)(NO_3)(H_2O)_2]$ (bptm = 1,1-bis(5-(pyrazin-2-yl)-1,2,4-triazol-3-yl) methane) is synthesized and characterized by IR spectroscopy and single crystal X-ray diffraction. Its reactivity with calf thymus DNA and HeLa cell DNA is measured using UV absorption and fluorescence spectroscopies. Gel electrophoresis assay demonstrates the ability of the complex to cleave pBR322 plasmid DNA. Eventually, the complex can suitably dock with a special DNA.

DOI: 10.26902/JSC20170812

K e y w o r d s: Pb complex, DNA binding, biological activity.

INTRODUCTION

Compounds with N-donor heterocycles are widely abundant in nature [1, 2]. The bases of hemoglobin and chlorophyll and nucleic acids that play an important role in plants and animals are compounds with N-donor heterocycles [3, 4]. They have been actively used in separation and extraction of metal ions, antibacterial and antitumor drugs, nucleic acid probe, magnetic resonance imaging, diagnosis and treatment of radioactive poisoning [5, 6]. A nitrogen heterocyclic compound and its derivatives introduced into organic compounds usually caused an increase in the biological activity of organic compounds, which enhances their performance and practical value. It has become a hot topic in the field of drug research and development [7, 8]. Lead has been well known to be toxic for the growth of organisms and its most preferred targets in organisms are sulfur-rich proteins and their zinc-binding sites. Lead substitution for zinc disrupts the structures of these proteins, making them dysfunctional.

In the last few decades, the coordination chemistry of Pb with hetero-donor ligands has remained an active area of research due to their interesting bonding modes. A wide range of Pb coordination numbers in such complexes has been reported [9—12]. Pb complexes have bio-relevant importance. In organisms, some metal ions can change the structure of DNA and thus affect the genetic information of DNA; therefore, it is necessary to study the interactions of Pb ions with DNA. Meanwhile, the search for low molecular weight molecules capable of catalytically cleaving DNA has attracted much interest among scientists, although a great number of nucleases are well-known [13—16]. All of these inspire us to further study the Pb complex [9, 17, 18]. This interest embraces the elucidation of the cleavage mechanism, the role of metals in biological systems, and the design of more effective synthetic hydrolases, as well as the use of these new compounds as catalysts, conformational probes, and synthetic restriction enzymes.

In this paper, we report the preparation, structures and DNA binding properties of a new metal complex chelated by 1,1-bis(5-(pyrazin-2-yl)-1,2,4-triazol-3-yl) methane, named [Pb(bptm)(NO_3)× ×(H_2O)$_2$]. The complex was characterized using elemental analysis, infrared (IR) spectroscopy, and single crystal X-ray diffraction. Furthermore, the DNA binding properties of the complex were investigated using UV absorption and fluorescence spectroscopies and gel electrophoresis.

EXPERIMENTAL

Materials and physical measurements. All chemicals and reagents purchased were of reagent grade and used without further purification unless otherwise noted, and distilled water was used. Fish Sperm DNA and pBR322 plasmid DNA were purchased from China. HeLa cell DNA implemented here we extracted ourselves. Elemental analysis (C, H and N) was performed on a model Finnigan EA 1112. The IR spectra were obtained as KBr pellets on a Nicolet FT-IR 470 spectrometer. UV-visible (UV-Vis) spectra were recorded on Shimadzu UV-240. Fluorescence measurements were carried out on a PerkinElmer LS55 fluorescence spectrofluorometer.

Synthesis of [Pb(bptm)(NO_3)(H_2O)$_2$]. An aqueous solution (10 ml) containing 0.11 mmol of bptm was added dropwise into a water solution (20 ml) of $Pb(NO_3)_2$ (0.1 mmol) with stirring. The mixture was heated at 70 °C for 72 h and gradually cooled to room temperature at a rate of 5 °C/h^{-1} to obtain colorless block-shaped crystals. Yield: 46 %. Anal. calc. for [Pb(bptm)(NO_3)(H_2O)$_2$] (%): C 25.53, H 2.14, N 25.21. Found, %: C 25.55, H 2.13, N 25.22. IR (KBr, cm^{-1}; w is weak; m is medium; s is strong)): 1384(s), 1145(m), 1026(m), 825(m),722(m), 1559(m), 1599(m), 1069(w), 1538(w), 853(w),761(w), 619(w), 527(w), 470(w).

X-ray crystal structure determination. Data for the [Pb(bptm)(NO_3)(H_2O)$_2$] complex was collected using a Bruker Smart 1000 CCD X-ray single crystal diffractometer with MoK_α radiation (λ = 0.71073 Å) at 273 K in ranges 2.38 < h < 25.15°. The structure was solved by direct methods and refined by means of full-matrix least-squares procedures with SHELXTL 97 systems. All non-hydrogen atoms were refined anisotropically. Hydrogen atoms were located from different Fourier maps.

DNA BINDING AND CLEAVAGE

UV-visible spectra is an accurate determination of the molecular structure of organic compounds. To understand the physical world at the molecular level, it is very important to promote the development of modern organic chemistry. Using modern instrument analysis, the method can quickly and accurately determine the molecular structure of organic compounds. UV-visible spectra were recorded on a Shimadzu UV-240. Tris-HCl buffer (pH 7.0) and a buffer (10 mmol/L) solution of complex was titrated with a concentrated Fish sperm DNA (FSDNA) solution.

Fluorescence spectra. For all fluorescence measurements, the entrance and exit slits were maintained at 15 nm and 15 nm, respectively. Samples were excited at 526 nm and emission was observed at 617 nm. The buffer used in the binding studies was 50 mM Tris-HCl (pH = 7.2) containing 10 mmol NaCl. Samples were incubated for 4 h at room temperature (20°C) before spectral measurements. Under these conditions, the fluorescence intensity of the respective complexes, extracted HC-DNA, and ethidium bromide (EtBr) was very small and could be ignored. The interaction of the respective complexes with DNA *in vitro* was studied as described in the literature [19—21].

Gel electrophoresis experiments were performed as described earlier [22]. Supercoiled pBR322 DNA (0.33 mg/ml^{-1}) was treated with metal complexes in the Tris buffer (50 mmol Tris-acetate, 18 mmol NaCl; pH = 7.2) and the mixtures were incubated for 1.5 h at room temperature. The samples were electrophoresed for 1.5 h at 90 V on 0.8 % agarose gel in the Tris-acetate buffer. After electrophoresis, the gel was stained with 1 mg/ml^{-1} EtBr and photographed under UV light.

Cell line and culture. The cell lines used in this experiment were routinely maintained in a RPMI-1640 medium supplemented with 10 % (v/v) heat inactivated fetal bovine serum, 2 mmol/l^{-1} of glutamine, 100 μg/ml^{-1} of penicillin, and 100 μg/ml^{-1} of streptomycin in a highly humidified atmosphere of 95 % air with 5 % CO_2 at 37 °C.

Apoptosis assays by flow cytometry. The ability of the complexes to induce apoptosis was evaluated using flow cytometry with Hela cell line using Annexin V conjugated with fluorescein isothiocyanate (FITC) and propidium iodide (PI) counterstaining. The cells in a usable condition were seeded in a 6-well culture plate at 1×10^6 cells per well in 3 ml of the culture medium. 12 and 24 h later, the complex was added to the medium respectively. After 12 h (24 h) incubation, the cells were gathered, and washed twice with cold phosphate-buffered saline. Then the cells were resuspended in 1×binding buffer at a concentration of 1×10^6 cells/ml^{-1}. An amount of 100 μl of the solution (1×10^6 cells) was transferred to a 5 ml culture tube and heat shocked at 60 °C for 5 min. Amounts of 5 μl of FITC-Annexin V and 5 μl of PI were added into the solution; the cells were incubated at room temperature (25 °C) in the dark for 15 min, and then 400 μl of 1×binding buffer was added to each tube. Final analysis was conducted using flow cytometry (Accuri C6, USA) within 1 h (a mesh filter being added before sample introduction).

RESULTS AND DISCUSSION

Structure of the complex. The crystal structure of the complex was determined using X-ray crystallography. The crystal data and structure refinement are presented in Table 1. The single crystal X-ray analysis reveals that the complex crystallizes in a monoclinic crystal lattice with the space group $P2_1/c$. The atomic numbering scheme and atom connectivity for the complex are shown in Fig. 1. The molecular structure of the complex reveals that Pb is six-coordinated by two nitrogen atoms from a bptm ligand, two oxygen atoms from two different intramolecular water molecules, and one oxygen from the nitro group. The Pb—O distance is 2.448(6) and the Pb—N distances are 2.434(6)—2.505(6) Å. Free water act as a hydrogen donor to form intermolecular hydrogen bonds with oxygen atoms of nitrato groups in the adjacent molecules. A three-dimensional structure is formed by O(2)—H(1W)···O(5) and O(2)—H(2W)···O(4) hydrogen bonds (Fig. 2). Their distance is 2.0168(810) and 2.0331(804).

Table 1

Crystal data and structural refinement for $[Pb(bptm)(NO_3)(H_2O)_2]$

Parameter	Complex
Empirical formula	C13 H13 N11 O5 Pb
Formula weight	610.53
Crystal system	Monoclinic
Space group	$P2(1)/c$
a, b, c, Å; β, deg.	12.6585(5), 8.5563(3), 17.3256(7); 98.2490(10)
Volume, Å^3	1857.12(12)
Z; calculated density, g/sm^{-3}	4; 2.184
Mu, mm^{-1}	9.140
F(000)	1160
Crystal size, mm	0.22×0.20×0.18
θ range for data collection, deg.	2.38 to 25.15
Limiting indices	$-14 \le h \le 15$, $-10 \le k \le 7$, $-20 \le l \le 19$
Reflections collected / unique	11611 / 3312 [R(int) = 0.0429]
Data completeness, %	99.6
Max. and min. transmission	0.2900 and 0.2383
Data / restraints / parameters	3312 / 37 / 286
Goodness-of-fit on F^{-2}	1.161
Final R indices [$I > 2\sigma(I)$]	$R_1 = 0.0361$, $wR_2 = 0.0977$
R indices (all data)	$R_1 = 0.0415$, $wR_2 = 0.1020$
$\Delta\rho_{max}$ / $\Delta\rho_{min}$, e/Å^3	1.866 / –2.085

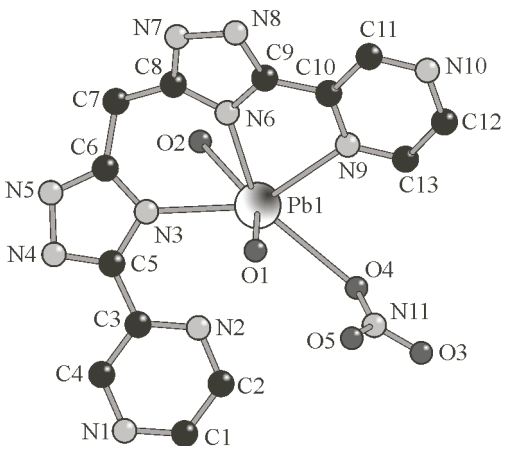

Fig. 1. Coordination environment of $[Pb(bptm)(NO_3)(H_2O)_2]$

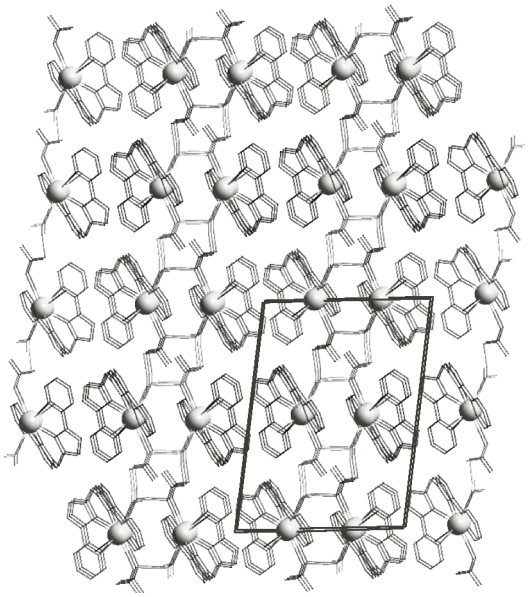

Fig. 2. 3D structure formed by O(2)—H(1W)…O(5) and O(2)—H(2W)…O(4) hydrogen bonds

UV absorption spectroscopy. The absorbance of the solution at 285 nm was initially measured for the complex after each addition of FS-DNA. It can be found that the wavelength red shift is as high as 16 nm, which verifies the existence of a strong electron feedback and a coordination effect between the ligands (Fig. 3). The greatest feature of all the UV absorption spectra is the aromatic nitrogen base coordination in π—π* electronic transition complexes. The formation of the intramolecular charge transfer spectral wavelength is relatively long, belonging to the MLCT spectrum, where the absorption intensity is weaker than the π—π* interaction. When the complex is doped into DNA, the characteristic absorption peak is red-shifted; at the same time the hypochromic effect was obviously excited. The complex bound with DNA by insertion and DNA spiral base pairs with the electron stack effect occurred, because two π orbitals from the ligand and DNA base pairs coupled, the energy declined, resulting in the red-shift phenomenon. At the same time, due to the partial filling with electrons, the coupling orbital make the π—π* transition probability decrease, producing the hypochromic effect.

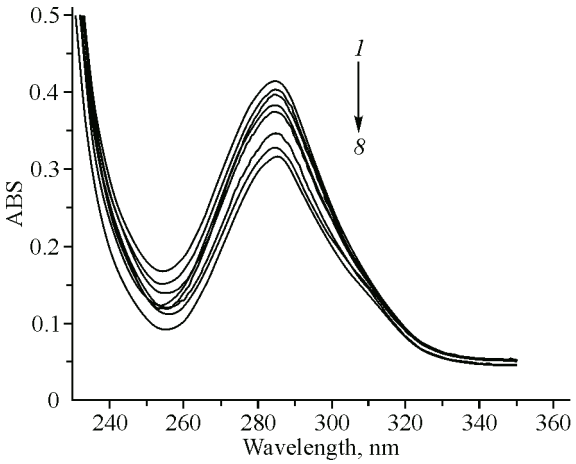

Fig. 3. Absorption spectra of the complex in 5 mmol Tris-HCl/NaCl buffer (pH = 7.0) in the absence (curve *1*) and presence (curves *2*—*8*) of increasing amounts of FS-DNA: 4, 8, 16, 20, 24, 32, 48 μM

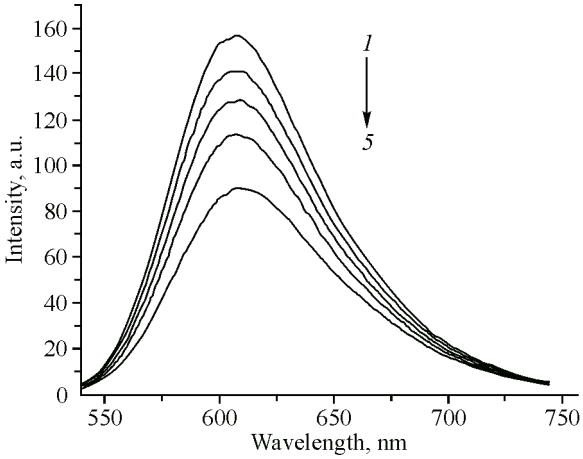

Fig. 4. Fluorescence spectra of the binding of EtBr to DNA in the absence (curve *1*) and presence (curves *2*—*5*) of increasing amounts of $[Pb(bptm)\times$ $\times(NO_3)(H_2O)_2]$

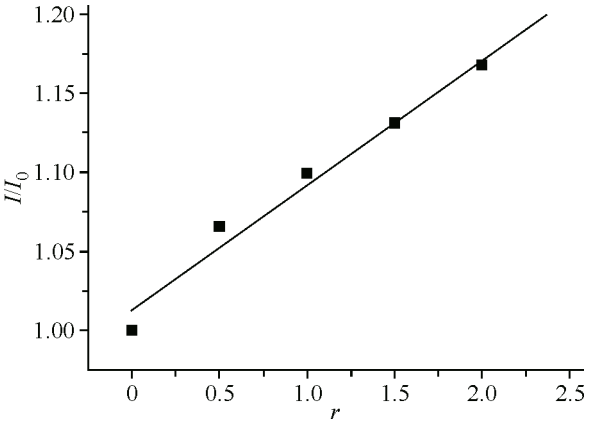

Fig. 5. Stern-Volmer quenching plots of [Pb(bptm)$(NO_3)(H_2O)_2$] with a slope of 0.0786

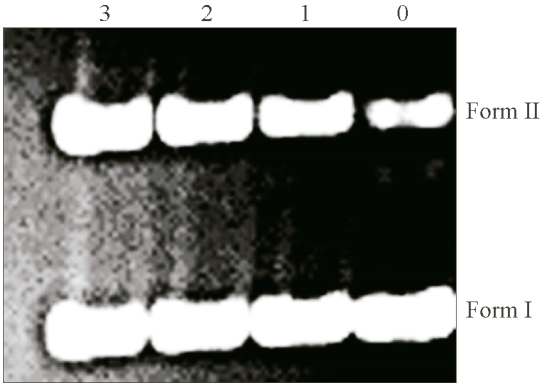

Fig. 6. Cleavage of pBR322 DNA (10 μM) in the presence of the complex: lane 0, DNA alone; lanes *1*—*3*, DNA+[Pb(bptm)$(NO_3)(H_2O)_2$] (14.0, 21.0,28.0 μM, respectively)

Fluorescence spectroscopy. EtBr is a conjugated planar molecule and can emit intense fluorescence in the presence of DNA due to its strong intercalation between the adjacent DNA base pairs. It was previously reported that the fluorescence could be quenched by the addition of complexes to DNA pretreated with EtBr, causing a reduction in the emission intensity, indicating that the complexes have displaced EtBr from DNA [23]. Liu et al. [24] found that the fluorescence quenching of EtBr-DNA by tetra-aza macrocyclic complexes might be due to the replacement of the DNA intercalator. The fluorescence emission spectra of EtBr bound to DNA in the absence and presence of [Pb(bptm)× ×$(NO_3)(H_2O)_2$] is shown in Fig. 4. Fluorescence intensities at 620 nm (526 nm excitation) were measured at various concentrations.

The classical Stern—Volmer equation is: $I_0/I = 1 + K_{sq}r$, where I_0 and I represent the fluorescence intensities in the absence and presence of the complex, respectively, r is the concentration ratio of the complex to DNA, and K_{sq} is a linear Stern—Volmer quenching constant dependent on the ratio of the EtBr bound concentration to the DNA concentration. The K_{sq} value is obtained as a slope of the linear plot of I_0/I versus r. The fluorescence quenching curves of DNA-bound EtBr for [Pb(bptm)(NO_3)× ×$(H_2O)_2$] is shown in Fig. 5.

Gel electrophoretic analysis. The degree to which the complex could function as a DNA cleavage agent was examined using supercoiled pBR322 plasmid DNA as the target. The cleavage efficiency was probed using agarose gel electrophoresis [25—27]. When circular plasmid DNA is investigated by electrophoresis, the fastest migration is observed for the supercoiled form (Form I). If one strand is cleaved, the supercoils relax to produce a slower moving nicked circular form (Form II). If both strands are cleaved, a linear form (Form III) is generated, which migrates in-between. The [Pb(bptm)$(NO_3)(H_2O)_2$] complex is found to promote the cleavage of pBR322 plasmid DNA from supercoiled Form I to nicked Form I (Fig. 6). The complex can induce an obvious cleavage of the plasmid DNA at a concentration of 1.25 μM. With increasing concentration of the complex (lanes *1*—*3*), the amount of Form I of pBR322 DNA diminishes gradually, whereas the amount of Form II increases. The complex exhibits a more effective DNA-cleavage activity.

Apoptotic study. The cell death mode was studied by Annexin-V/Propidium Iodide (PI) binding assay with the complex in HeLa cells. Respectively, in 12 and 24 h incubation of the cells and subsequent photo irradiation (400—700 nm, 10 cm^{-2}) caused about 65 % of the cells to undergo apoptosis. They are shown in Fig. 7. The figures suggest that the number of dead cancer cells increases gradually with time in early apoptotic (lower right quadrant) or late apoptotic/necrotic(upper right quadrant). Morphological features of apoptotic and viable HeLa cells stained with Annexin V-FITC and Propidium Iodide(PI), the experiment is repeated by reproducing the conditions as nearly as possible, under confocal fluorescence images of HeLa cells. The result is depicted in Fig. 8.

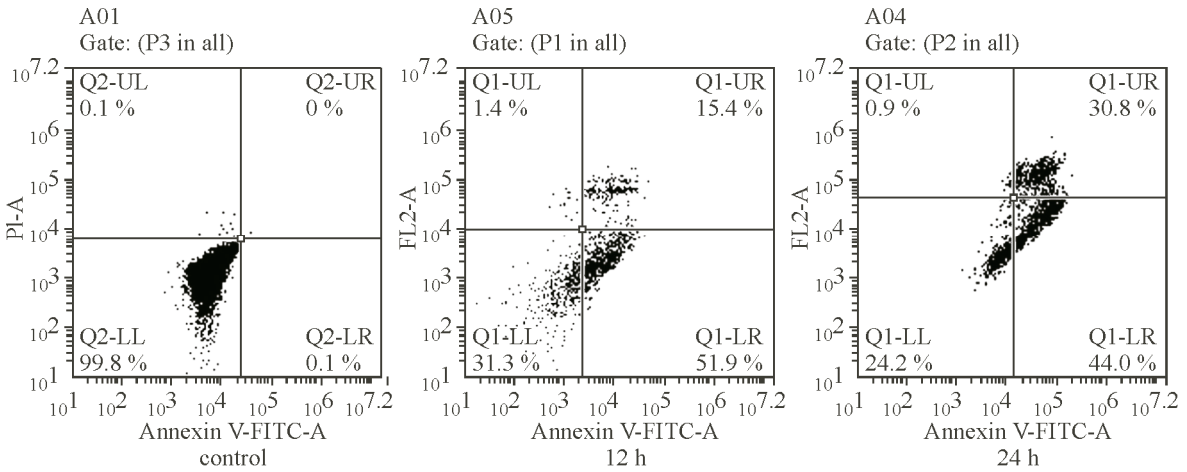

Fig. 7. Hela cells cultured with or without 1000 mg/ml of [Pb(bptm)(NO_3)(H_2O)$_2$] for 12 and 24 h were measured by surface expression of phosphatidyl serine using FITC-Conjugated Annexin-V antibody. Membrane permeability was assessed by propidium iodide exclusion (PI) analyzed by flow cytometry

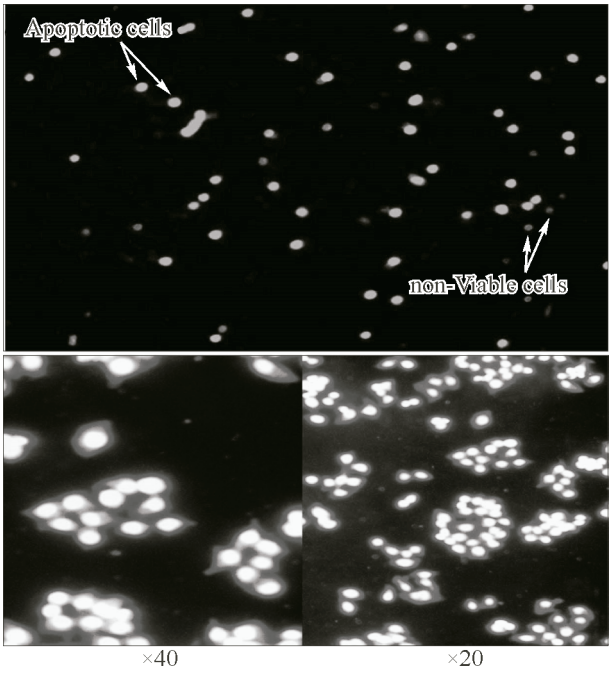

Fig. 8. Apoptosis in Hela cells at exposure to 6.7 μM of [Pb(bptm)(NO_3)(H_2O)$_2$] for 12 h and stained with Annexin-V FITC/PI. The morphology of the Hela cells was observed by the microscope

CONCLUSIONS

We described the synthesis and characterization of the [Pb(bptm)(NO_3)(H_2O)$_2$] complex. The crystal structure of the complex was determined by single crystal X-ray diffraction. The UV-visible and fluorescence spectral study was used to investigate the binding of the complex with fish sperm DNA. Gel electrophoretic analysis demonstrated the ability of the complex to cleave the pBR322 plasmid DNA.

We gratefully acknowledge the Natural Science Foundation of China (No. 21171118 and No. 21671138), the Distinguished Professor Project of Liaoning province.

REFERENCES

1. *Ramos A.P. et al.* // Dalton Trans. – 2015. – **44**, N 8. – P. 3829 – 3836.
2. *Cirera J., Babin V., Paesani F.* // Inorg. Chem. – 2014. – **53**, N 20. – P. 11020 – 11028.
3. *Dani R.K. et al.* // Polyhedron. – 2014. – **81**. – P. 261 – 272.
4. *Wei Y.L. et al.* // Inorg. Chem. Commun. – 2002. – **5**, N 2. – P. 166 – 170.
5. *Lahoud M.G. et al.* // Polyhedron. – 2013. – **54**. – P. 1 – 7.
6. *Tian J.M. et al.* // Crystengcomm. – 2014. – **16**, N 6. – P. 1071 – 1078.
7. *Wang X.H. et al.* // Chem. Commun. – 2011. – **47**, N 28. – P. 8127 – 8129.
8. *Wang J. et al.* // J. Struct. Chem. – 2013. – **54**, N 3. – P. 555 – 559.
9. *Chakraborty S. et al.* // Molecules. – 2013. – **18**, N 5. – P. 4972 – 4985.
10. *Mahmoudi G. et al.* // Dalton Trans. – 2016. – **45**. – P. 4965 – 4969.
11. *Chen, Y.T. et al.* // Crystengcomm. – 2015. – **17**, N 10. – P. 2129 – 2140.
12. *Wu Y.L. et al.* // J. Solid State Chem. – 2015. – **223**. – P. 131 – 137.
13. *Zhao P. et al.* // Spectrochim. Acta A Mol. Biomol. Spectroscop. – 2008. – **71**, N 4. – P. 1216 – 23.
14. *Loganathan R. et al.* // Inorg. Chem. – 2012. – **51**, N 10. – P. 5512 – 5532.
15. *Patel M.N., Joshi H.N., Patel C.R.* // J. Chem. Sci. – 2014. – **126**, N 3. – P. 739 – 749.
16. *Chen M.-Z. et al.* // Chem. & Pharmaceutical Bulletin, 2013. – **61**, N 7. – P. 714 – 721.
17. *Ravichandran R., Rajendran M., Devapiriam D.* // J. Coord. Chem. – 2014. – **67**, N 8. – P. 1449 – 1462.
18. *Ni R. et al.* // Macromolecules. – 2008. – **41**, N 14. – P. 5477 – 5484.
19. *Tripathy S.K. et al.* // Dalton Trans. – 2015. – **44**, N 11. – P. 5114 – 5124.
20. *Taylor, J.A. et al.* // Nucl/ Acids Res. – 2015. – **43**, N 2. – P. 719 – 731.
21. *N'Soukpoe-Kossi C.N. et al.* // DNA and Cell Biology. – 2008. – **27**, N 2. – P. 101 – 107.
22. *Sannohe Y., Sugiyama H.* // Bioorganic & Medicinal Chemistry. – 2012. – **20**, N 6. – P. 2030 – 2034.
23. *Crnolatac I. et al.* // Chemmedchem. – 2013. – **8**, N 7. – P. 1093 – 1103.
24. *Yang J. et al.* // Crystal Growth & Design. – 2014. – **14**, N 12. – P. 6521 – 6527.
25. *Srivastava A.K. et al.* // Indian J. Chem. Section a-Inorganic Bio-Inorganic Phys. Theoretical & Analyt. Chem. – 2013. – **52**, N 7. – P. 835 – 844.
26. *Vujcic M. et al.* // J. Biochem. Mol. Toxicology. – 2011. – **25**, N 3. – P. 175 – 182.
27. *Gumus F. et al.* // J. Medicinal Chem. – 2009. – **52**, N 5. – P. 1345 – 1357.